E.M.B. Heller [a,*], J.F. Suyver [a], A.M. Vredenberg [a], D.O. Boerma [a,b]

[a] *Debye Institute, Section Interface Physics, Utrecht University, P.O. Box 80.000, 3508 TA Utrecht, Netherlands*
[b] *Department of Nuclear Solid State Physics, Materials Science Center, Groningen University, Nijenborgh 4, 9747 AG Groningen,
Netherlands*

Abstract

The hydrogen storage material FeTi has the disadvantage to lose its sorption capacity in contact with impurities such as O_2 and H_2O. A possibility to overcome this problem is to coat it with an anti-corrosive layer which is permeable for hydrogen. In this study we prepared FeTi layers covered with a (4 or 20 nm) thin Pd layer. We used ion beam and sputter profiling techniques, X-ray photoelectron spectrometry and scanning probe techniques to investigate the response of these bi-layers upon annealing up to 300°C in vacuum, air and 10^{-5} mbar O_2. The layered structure remains intact up to 150°C. At 200°C in air and O_2, Fe and (some) Ti move towards the Pd surface where they form oxide regions. At higher temperatures thicker oxide regions, presumably along the Pd grains, are formed. These processes are more pronounced for the case of 4 nm Pd. A model is presented to explain the observed phenomena. We conclude that up to 150°C 4 nm of Pd is sufficient to act as a protective layer. For a temperature of 200°C, 20 nm Pd may still provide sufficient protection against oxidation. © 1999 Elsevier Science B.V. All rights reserved.

1. Introduction

The intermetallic compound FeTi is a promising material for reversible hydrogen storage. In the FeTi matrix, 37% more hydrogen per unit volume can be stored than is contained in liquid hydrogen [1]. In comparison with other hydrogen storage materials, FeTi has the advantage to store and release hydrogen at useful pressures (around atmospheric pressure) and temperatures (around room temperature). However, this material is highly corrosive. In addition, embrittlement and a necessary activation treatment prior to hydrogen charging are major drawbacks.

The oxidation of FeTi due to previous air exposure or impurities of H_2O and O_2 during cycling with hydrogen is seen as the reason for the necessary activation [2]. The activation treatment normally consists of a vacuum or hydrogen anneal at high temperatures. As a result of this treatment the surface oxide layer, which hinders hydrogen absorption, is resolved in metallic Fe and TiO_2. During subsequent

* Corresponding author. Fax: +31-30-254-3165; E-mail: e.m.b.heller@phys.uu.nl

loading, the atomic hydrogen can be absorbed after dissociation at Fe [3]. In order to prevent impurities (H_2O and O_2) to reach the reactive surface we applied a coating of Pd, as was suggested by Sanders [4]. A possible additional advantage is that Pd coating [5] or alloying is beneficial for hydrogen uptake [6]. Embrittlement is the result of the swelling and shrinking processes that are associated with the charging and discharging cycles. In principle, the problem of embrittlement can be overcome by using FeTi in the form of a powder with grain sizes of a few μm diameter. As a storage system, one could think of a structure composed of finely dispersed FeTi particles which are attached to an inert support and covered by a thin Pd coating.

In this paper, we present results on the oxidation behavior of FeTi covered with a layer of Pd in the temperature range of the hydrogen loading and release. We used a layered structure as a model system for a storage system based on small particles. Next to several ion beam techniques to monitor compositional changes in the film and to determine the amount of O uptake, we used X-ray Photoelectron Spectroscopy (XPS) to characterize the chemical state of the elements present in the first few nm of the surface. We studied the properties of the protective layer for two different thicknesses of the Pd layer, 4 and 20 nm, in order to determine its usefulness as a protective layer against oxidation.

2. Experimental

Bi-layers of FeTi/Pd on Si wafers were prepared with e-beam physical vapour deposition at a background pressure of 6×10^{-8} mbar. The FeTi layer was evaporated from a mixture of 99.7% FeTi (TiMet) combined with 99.9% Ti (Balzers) in a weight ratio of 1:6. The admixture of Ti was needed to obtain an Fe/Ti film composition close to 50/50. The Pd layer was evaporated from 99.99% Pd buttons (Balzers). During all evaporations the pressure in the preparation chamber stayed below 5×10^{-7} mbar. The layer thickness and composition were determined with Rutherford Backscattering Spectrometry (RBS) using a 2.7 MeV He$^+$ beam. We used a scattering angle of 170°, with the beam

making an angle of 60° with the surface normal. From RBS on 'as deposited' samples, it followed that the FeTi layer had an Fe/Ti atomic ratio of 55/45 and a thickness of 90 nm. RBS spectra were analyzed using the computer code RUMP [7].

Depth profiles of C, N, O were measured with Elastic Recoil Detection (ERD), using an incoming beam of 72 MeV Ag ions, at an incident angle of 25° with respect to the surface plane. Outcoming particles were detected in a δE–E telescope [8] at a recoil angle of 50°. The scattering plane was perpendicular to the surface. Contamination levels of C, N and O in the FeTi/Pd layer were below 0.5 at.%. The H content of 'as deposited' layers was 1 and 3 at.% in the FeTi and Pd layer, respectively.

X-ray Diffraction (XRD) of the 'as deposited' FeTi/Pd showed Pd lines, indicating the presence of polycrystalline Pd. No FeTi, Fe_2Ti, Ti, or Fe lines were observed. The FeTi layer is most probably amorphous or nano-crystalline.

XPS was used to analyze the chemical state of the elements present in the first 10 nm of the surface. XPS was done using a CLAM-2 hemispherical sector analyzer and an Al K_α source. On the surface of 'as deposited' layers, only metallic Pd, as well as C and O were observed. This implies that the Pd layer fully covers the FeTi. To further analyze the depth profiles, sputtering Auger Spectroscopy was performed at Groningen University using a JEOL JAMP 7800 F with a primary beam of 10 keV and a probing diameter of 100 nm. Sputtering was done with Ar.

The surface morphology of the samples was inspected with Atomic Force Microscopy (AFM) and Scanning Electron Microscopy (SEM) after various annealing steps. With SEM, the surface of the 'as deposited' sample appeared featureless, while with AFM no structure down to the scale of 1 nm could be discerned.

FeTi/Pd bi-layers were subjected to controlled heating in 1×10^{-5} mbar, in air, and in vacuum (1×10^{-9} mbar) in the temperature range of 150–300°C during 1 h. The anneals in 1 atm air were performed in an open tube-furnace. All XPS scans were done in the same system as used for the vacuum and O_2 anneals. No interdiffusion was observed with RBS before or after the treatments between the FeTi layer and the Si substrate.

3. Results

3.1. 20 nm Pd coating: vacuum annealing

Samples consisting of 20 nm Pd on FeTi were annealed at 150, 200 and 300°C in vacuum for 1 h. Fig. 1 shows the RBS spectra of the FeTi and the Pd layer. The surface energies of the elements are indicated in the picture. No difference was observed in spectra taken before and after annealing at 150°C. In these spectra we observe at the surface a clear Pd signal and no Fe signal. This implies that the Pd layer fully covers the FeTi. This is confirmed by XPS measurements, in which we observe no Fe signal after the 150°C anneal (Fig. 2). After annealing at 200°C, in the depth range of the Pd, an Fe concentration with a mean value of 1 at.% and decreasing towards the surface is inferred from the RBS spectra (see Fig. 1). At 300°C, the near-surface Fe signal is flat (with a corresponding concentration of 5 at.%). In both cases, this is an indication that Fe diffuses into the Pd layer, probably along grain boundaries. In this process, the Pd layer may break up in grains separated by FeTi, such that the FeTi is visible for the ion beam.

In situ XPS measurements in Fig. 2 show that after vacuum annealing at 200 and 300°C, Fe is near the surface. Comparison with reference spectra leads
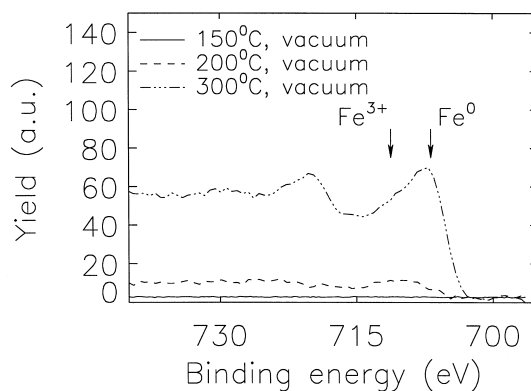

Fig. 2. XPS Fe(2p) spectra of 20 nm Pd on FeTi annealed in vacuum.

to the conclusion that most of the Fe is metallic and only a small fraction of the Fe signal is due to Fe-oxide. ERD spectra of all vacuum annealed samples show no increase in the O content in the Pd or FeTi layer. The O contents in the total layer after each treatment is given in Fig. 3.

AFM images of the FeTi/Pd layer annealed at 200°C (see Fig. 4a) indicate that the roughness of the layer increases with temperature. After annealing at 200°C, spherical bumps with a diameter of around 15
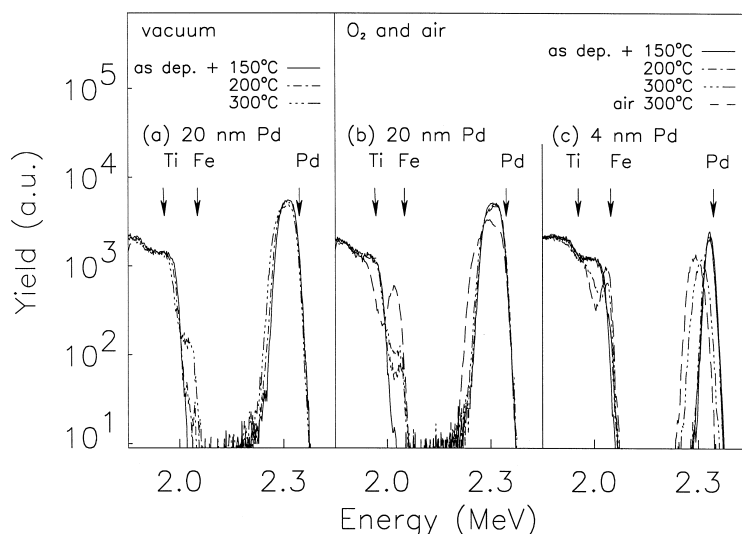

Fig. 1. RBS profiles of 20 nm Pd (a and b) and 4 nm (c) on FeTi 'as deposited' and after several anneals. The spectrum of FeTi/Pd annealed at 150°C has full overlap with the spectrum of the 'as deposited' layer. Note that a logarithmic scale is used to make visible small changes. The energies corresponding to scattering from the elements at the surface are indicated with arrows.
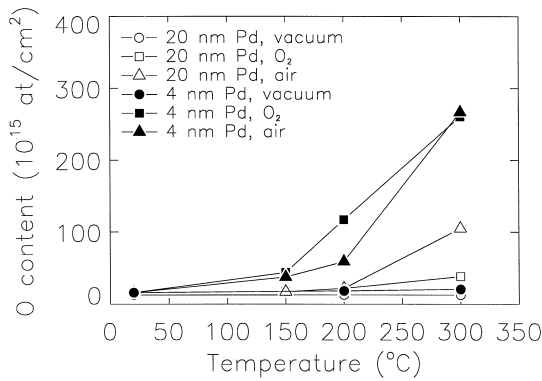
Fig. 3. O contents in the entire FeTi/Pd layer from ERD and RBS measurements on 4 and 20 nm Pd on FeTi annealed in vacuum, 1×10^{-5} mbar O_2 and air.

nm and a 4 to 5 nm height are observed on a smooth surface.

3.2. 20 nm Pd coating: annealing in O_2 and air

FeTi/Pd samples were annealed at 150, 200 and 300°C in 1×10^{-5} mbar O_2 or 1 atm air for 1 h. The RBS spectra, shown in Fig. 1, do not show an observable change between the 'as deposited' sample and the sample annealed at 150°C (Fig. 1). This implies that the composition and layered structure of the samples remain intact up to 150°C, the same as with vacuum annealing. XPS measurements confirm this (see Fig. 5). From Fig. 1, it is clear that starting from 200°C again Fe appears at the surface. At 200°C, the corresponding fraction is 3 at.% Fe for O_2-annealed samples. After annealing at 300°C more Fe is found near the surface: for O_2 anneals the
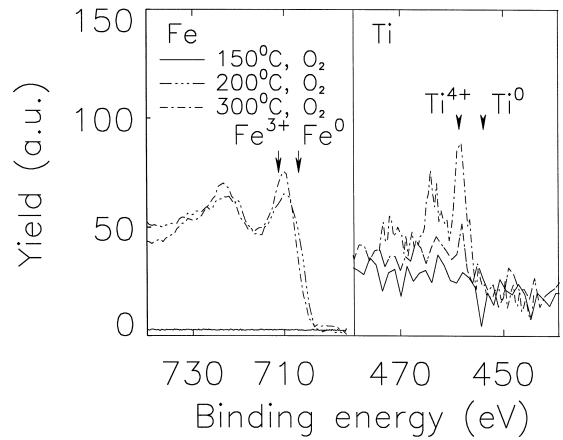

Fig. 5. XPS spectra of samples annealed in 1×10^{-5} mbar O_2 with 20 nm Pd on FeTi. The Fe(2p) (left) and Ti(2p) (right) regions are shown. Similar spectra were obtained after annealing in air.

corresponding Fe fraction in Pd is 5 at.%; for air anneals a large Gaussian shaped Fe peak is found at the surface. In the latter case the Pd peak has decreased and has become much broader, now peaking at larger depths. From comparison of the spectra to simulations one can derive that, in contrast with the O_2-annealed sample, the layer structure has changed over at least 45 nm.

From the O region in the RBS spectrum (not shown), it appears that a large amount of O is incorporated in the sample. From the XPS measurements (Fig. 5) it can be derived that at and above 200°C Fe_2O_3 forms near the surface. Also TiO_2 is detected. In the left hand side of Fig. 6, the depth
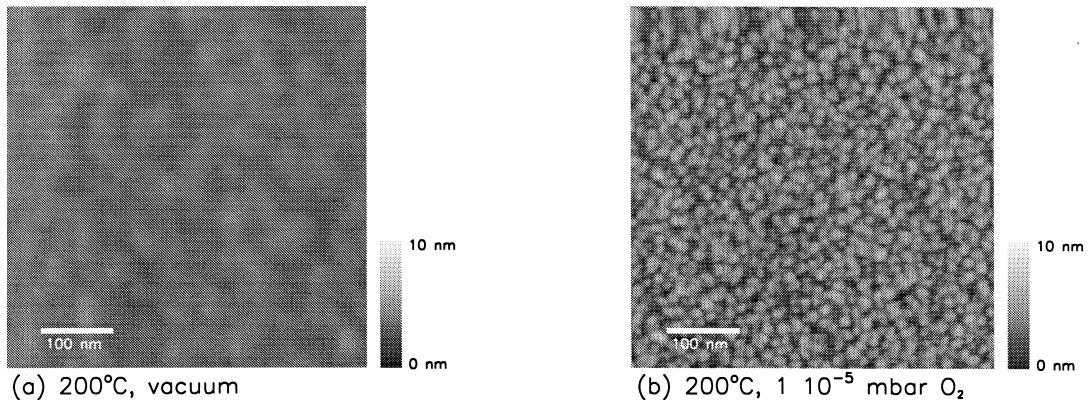

(a) 200°C, vacuum

(b) 200°C, 1 10^{-5} mbar O_2

Fig. 4. AFM picture of 20 nm Pd on FeTi annealed at 200°C: in vacuum (a) and in 1×10^{-5} mbar O_2 (b).
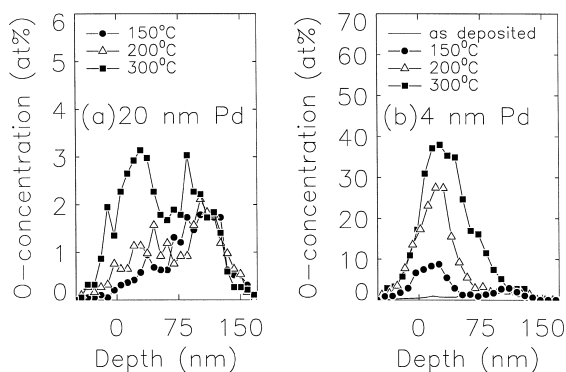
Fig. 6. ERD O profiles of 20 (left) and 4 nm Pd (right) on FeTi 'as deposited' and annealed in 1×10^{-5} mbar O_2. For 20 nm Pd, the O profile of the 'as deposited' layer is essentially the same as the profile of the layer annealed at 150°C.

Fig. 7. Auger peak-to-peak values of the differentiated spectrum during sputtering of 20 nm Pd on FeTi annealed in 1×10^{-5} mbar O_2 at 200°C. The sputtering rate was 1.5 nm/min.

profiles of O measured with ERD are shown for O_2-anneals. The peak centered around 90 nm is present in all samples and is due to a thin native Si-oxide at the interface. The O content in the FeTi is approximately 0.5 at.% after deposition. After annealing at 200°C in O_2 some extra O is observed as a peak near the surface position. Because the sample may have become rough, it is not possible to decide whether this O is at or near the surface. Roughness is indeed observed in AFM images taken from the same sample, as shown in Fig. 4b. The surface has changed drastically from smooth before annealing to granular after annealing. The grain sizes are in the order of 10 nm in diameter and 6–7 nm in height.

The presence of O at the surface was confirmed by Auger sputter profiling. Fig. 7 shows the Auger sputter profile of the sample annealed at 200°C in O_2, taken with a beam with a diameter of 100 nm. Besides Pd, Fe, Ti and O are present at the surface. The O profile decreases to zero after 3 min of sputtering and remains zero, indicating the presence of a surface oxide. Deeper in the sample a low level of Fe and Ti can be seen next to a high level of Pd. When the Pd decreases both the Fe and Ti increase, marking the end of the Pd top layer.

3.3. 4 nm Pd coating: vacuum annealing

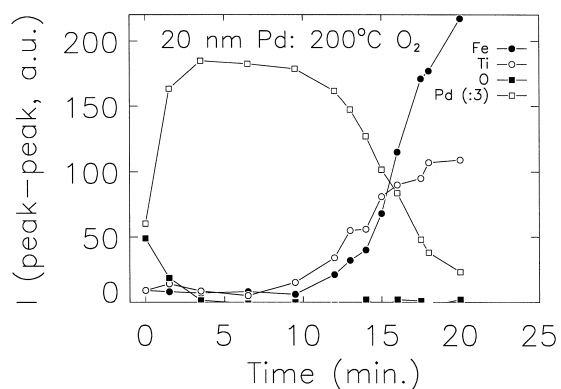FeTi samples coated with 4 nm Pd showed the same trend in compositional change after vacuum

annealing at temperatures of 150, 200 or 300°C, as the ones coated with 20 nm Pd. Both RBS and XPS measurements showed this. The O content of these layers remained low, as can be seen in Fig. 3.

3.4. 4 nm Pd coating: annealing in O_2 and air

In Fig. 1c, the RBS spectra of annealing in O_2 and air are shown. Up to 200°C, the trend is very similar to the 20 nm case. Again, some Fe is seen at the surface, although it is more than with 20 nm Pd. Annealing at 300°C in O_2 or air changes the near-surface composition drastically. An Fe peak is ob-
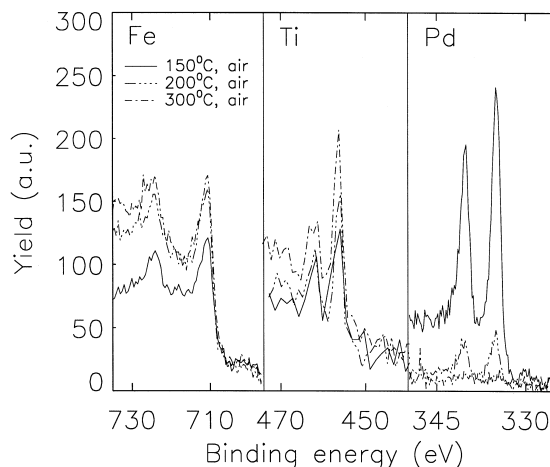

Fig. 8. XPS spectra of 4 nm Pd on FeTi annealed in air. From left to right, the Fe(2p), Ti(2p) and Pd(3d) regions are shown.
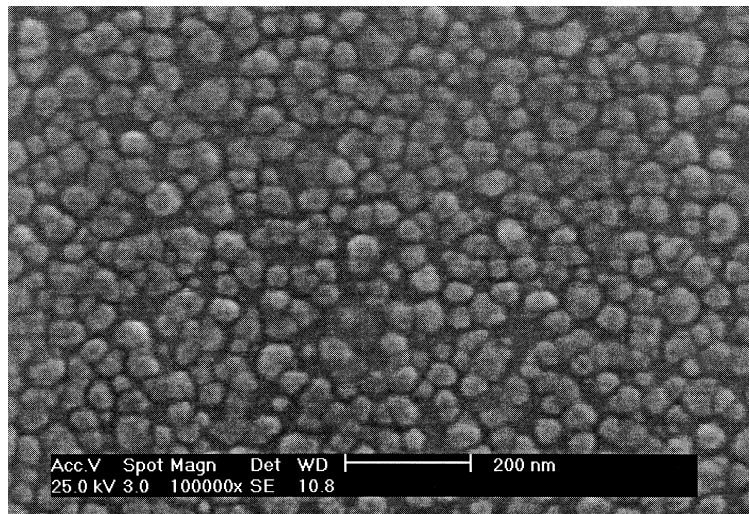
Fig. 9. SEM image of 4 nm Pd on FeTi annealed at 300°C in 1×10^{-5} mbar O_2.
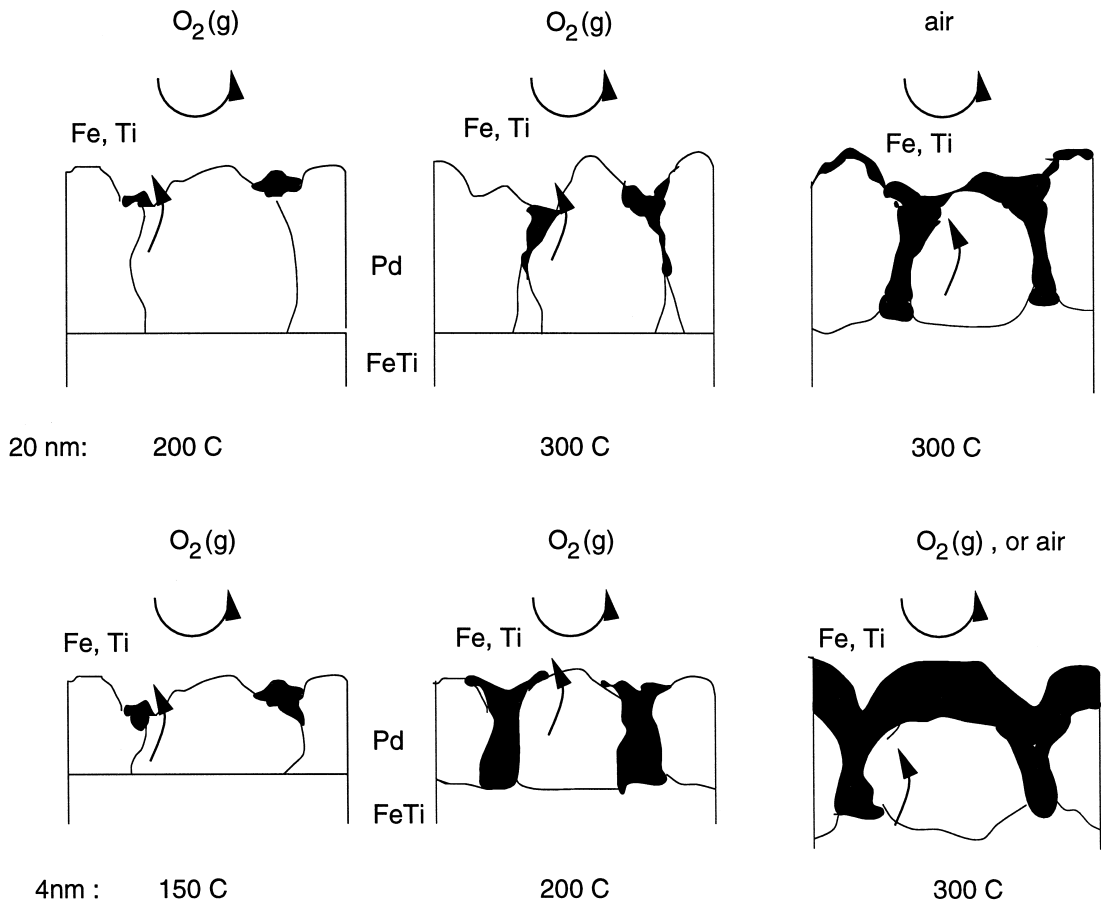

Fig. 10. Schematic representation of the proposed model for oxidation of FeTi/Pd bilayers. Top: 20 nm Pd, bottom: 4 nm Pd.

served at the surface, while the Pd peak broadens and shifts to a larger depth. This is similar to what is observed in the 20 nm air-annealed case. Apparently, with 4 nm Pd the same occurs also during O_2 annealing, although not as markedly as during annealing in air. Comparison to simulations indicate that on the 300°C air-annealed sample an FeTi-rich surface layer of around 2 nm has formed on top.

Above 150°C, the O content increases drastically with annealing in O_2, the effect being more pronounced at higher temperatures, as can be seen in the right hand side of Fig. 6. Annealing in air shows the same trend (see Fig. 3). XPS measurements, as shown in Fig. 8, clearly indicate the presence of Fe_2O_3 and TiO_2 near the surface. With higher annealing temperatures the Pd signal decreases, indicating either surface roughening or coverage of Pd by Fe or Ti. After annealing at 300°C in air, there is no Pd near the surface anymore (see Fig. 8), which confirms the RBS results in Fig. 1(c). The SEM image in Fig. 9, taken from the 300°C O_2-annealed sample, shows strong roughening, suggesting the formation of small particles with a diameter of 40–70 nm.

4. Discussion and conclusion

In this section, we try to explain the observations as described in Sections 2 and 3. Our explanation is inspired by observations and the description of the oxidation of a Fe layer covered with an epitaxial Ag layer with a thickness of 20 nm [9]. In Fig. 10, our interpretation of the observations is drawn schematically. At temperatures of 150–200°C, transport of Fe and some Ti along the grain boundaries in the Pd layer takes place. In the presence of O_2 or air oxidation occurs at the surface and a small amount of Fe and Ti oxidizes into Fe_2O_3 and TiO_2. At the same time the surface roughens. Upon annealing in O_2 at higher temperatures (200°C for 4 nm Pd and 300°C for a 20-nm Pd coating), further oxidation takes place through the same channels and regions of Fe- and Ti-oxide appear at the surface. In the case of 4 nm Pd, FeTi also oxidizes deeper. This process continues progressively. Finally, at 300°C (in air for

20 nm Pd, in O_2 or air for 4 nm Pd), thick oxide regions are formed along the Pd grains. In the case of 4 nm, the oxide starts to encapsulate the grains, covering them with a thin oxide layer.

This model explains the roughness we observed with AFM in samples annealed at temperatures above 200°C. The roughening and the appearance of Fe and Ti at the surface may be related phenomena. Due to the diffusion of Fe and Ti along grain boundaries in the Pd layer roughening may be enhanced. It should be noted that due to the resolution of the techniques used, the structures we describe in our model were to small to observe directly. The model is also consistent with the appearance of Fe- and Ti-oxide at the surface after annealing, which we observed with XPS and Auger depth profiling, as well as with the disappearance of the Pd signal in XPS measurements, and with the concentration profiles following from the RBS and ERD spectra.

In conclusion, up to 150°C, 4 nm of Pd is sufficient to act as a protective layer. For a temperature of 200°C, 20 nm Pd may still provide sufficient protection against oxidation, regardless the small amount of Fe- and Ti-oxide formed at the surface.

Acknowledgements

References

[1] J. Reilly, R. Wiswall Jr., Formation and properties of iron titanium hydride, Inorg. Chem. 13 (1974) 218.
[2] J. Sanders, B. Tatarchuk, Buried-interfacial reactivity of palladium coated Fe_2O_3 /FeTi thin films during vacuum or hydrogen annealing, J. Phys.: Condens. Matter 2 (1990) 5809.
[3] L. Schlapbach, T. Riesterer, The activation of FeTi for hydrogen absorption, Appl. Phys. A 32 (1983) 169.

[4] J. Sanders, B. Tatarchuk, Protection of FeTi thin films using palladium coatings, J. Phys. F: Met. Phys. 18 (1988) L67.

[5] L. Zaluski, A. Zaluska, P. Tessier, J. Strom-Olsen, R. Schultz, Catalytic effect of Pd on hydrogen absorption in mechanically alloyed Mg_2Ni, $LaNi_5$ and FeTi, J. Alloys Comp. 217 (1995) 295.

[6] S. Kulshreshtha, O. Jayakumar, K. Bhatt, Hydriding character-istics of palladium and platinum alloyed FeTi, J. Mater. Sci. 28 (1993) 4229.

[7] L. Doolittle, A semiautomatic algorithm for Rutherford backscattering analysis, Nucl. Inst. Meth. B (1986).

[8] W.M. Arnold Bik, F.H.P.M. Habraken, Elastic recoil detec-tion, Rep. Prog. Phys. 56 (1993) 859.

[9] A.V. Mijiritskii, unpublished.